Myeloperoxidase Deficiency Attenuates Lipopolysaccharide-Induced Acute Lung Inflammation and Subsequent Cytokine and Chemokine Production[1]

Astrid Haegens,* Peter Heeringa,† Robert Jan van Suylen,‡ Chad Steele,§ Yasuaki Aratani,¶ Robert J. J. O'Donoghue,‖ Steven E. Mutsaers,‖ Brooke T. Mossman,# Emiel F. M. Wouters,* and Juanita H. J. Vernooy[2]*

Lung neutrophilia is common to a variety of lung diseases. The production of reactive oxygen and nitrogen species during neutrophil oxidative burst has been associated with protein and DNA damage. Myeloperoxidase (MPO) is an enzyme stored in the azurophilic granula of neutrophils. It is important in host defense because it generates the reactive oxidant hypochlorous acid and has been described to play a role in the activation of neutrophils during extravasation. We hypothesized that MPO contributes directly to the development of acute lung neutrophilia via stimulation of neutrophil extravasation and indirectly to the subsequent production of cytokines and chemokines in the lung. To test this hypothesis, wild-type (WT) and *Mpo*$^{-/-}$ mice were given a single LPS instillation, after which the development of neutrophil-dominated lung inflammation, oxidative stress, and cytokine and chemokine levels were examined. *Mpo*$^{-/-}$ mice demonstrated a decreased lung neutrophilia that peaked earlier than neutrophilia in WT mice, which can be explained by decreased neutrophil chemoattractant levels in LPS-exposed *Mpo*$^{-/-}$ compared with WT mice. However, oxidative stress levels were not different in LPS-exposed WT and *Mpo*$^{-/-}$ mice. Furthermore, in vivo findings were confirmed by in vitro studies, using isolated neutrophils. These results indicate that MPO promotes the development of lung neutrophilia and indirectly influences subsequent chemokine and cytokine production by other cell types in the lung. ***The Journal of Immunology,*** **2009, 182: 7990–7996.**

Neutrophilia is a key player in lung disorders such as acute respiratory distress syndrome (1), idiopathic pulmonary fibrosis (2), and asbestosis (3). It's also a feature common to all stages of chronic obstructive pulmonary disease (4) and increased neutrophil levels are reported in induced sputum of chronic obstructive pulmonary disease patients during exacerbations (5).

Myeloperoxidase (MPO)[3] has been described as a protein with proinflammatory properties independent of its enzymatic activity contributing to neutrophil extravasation (6). We have recently reported data demonstrating a significant reduction of neutrophil influx in *Mpo* knockout (*Mpo*$^{-/-}$) mice compared with *Mpo*$^{+/+}$ wild-type (WT) mice after inhalation of the inflammatory fiber chrysotile asbestos (7). This clearly shows that MPO plays a critical role in the development of asbestos-induced lung inflammation.

In this study, we hypothesized that MPO contributes directly to the development of acute lung neutrophilia via stimulation of neutrophil extravasation and indirectly through the subsequent production of cytokines and chemokines in the lung. This hypothesis was tested by exposing *Mpo*$^{-/-}$ and WT mice to a single intratracheal instillation of LPS to induce transient lung inflammation.

The development of lung inflammation was examined by quantification of inflammatory cell influx and MPO activity. Oxidative stress was measured indirectly by *heme oxygenase 1* (*ho-1*) expression and cytokine and chemokine expression in lungs and bronchoalveolar lavage fluid (BALF) were investigated. Furthermore, in vivo findings were confirmed by in vitro studies using isolated neutrophils.

Our results show that LPS exposure results in a dramatic increase in MPO activity in WT mice. Neutrophil influx in response to LPS exposure is significantly decreased in *Mpo*$^{-/-}$ mice compared with WT mice, mainly due to the decreased migration capacity of *Mpo*$^{-/-}$ neutrophils. *Ho-1* expression levels increased after LPS exposure but similar levels were observed in WT and *Mpo*$^{-/-}$ mice. Last, LPS-exposed *Mpo*$^{-/-}$ mice demonstrated an altered pattern of IL-6, keratinocyte-derived chemokine (KC), MIP-1α, RANTES, IL-13, and IFN-γ in BALF compared with WT mice, which could not be explained by altered cytokine and chemokine production by *Mpo*$^{-/-}$ neutrophils in vitro. Our data support the role of MPO as a key player in neutrophil extravasation and suggest that MPO alters chemokine and cytokine production by resident lung cells that may govern inflammatory responses.

*Nutrition and Toxicology Research Institute Maastricht, Department of Respiratory Medicine, Maastricht uMC+, The Netherlands; †Department of Pathology, University Medical Center Groningen, Groningen, The Netherlands; ‡Department of Pathology, University Hospital Maastricht, The Netherlands; §Department of Medicine, University of Alabama, Birmingham, AL 35294; ¶International Graduate School of Arts and Sciences, Yokohama City University, Kanagawa, Japan; ‖Lung Institute of Western Australia, Western Australia, Australia; and #Department of Pathology, University of Vermont, Burlington, VT 05405

Received for publication February 11, 2008. Accepted for publication April 17, 2009.

The costs of publication of this article were defrayed in part by the payment of page charges. This article must therefore be hereby marked *advertisement* in accordance with 18 U.S.C. Section 1734 solely to indicate this fact.

[1] P.H. is supported by a grant from the Dutch Organization of Scientific Research (NWO VIDI Grant 917.66.341).

[2] Address correspondence and reprint requests to Dr. Juanita H. J. Vernooy, Department of Respiratory Medicine, Maastricht uMC+, PO Box 5800, NL-6202 AZ Maastricht, The Netherlands. E-mail address: j.vernooy@pul.unimaas.nl

[3] Abbreviations used in this paper: MPO, myeloperoxidase; BALF, bronchoalveolar lavage fluid; HOCl, hypochlorous acid; *ho-1*, *heme oxygenase-1*; KC, keratinocyte-derived chemokine; Q-PCR, quantitative PCR; WT, wild type.

www.jimmunol.org/cgi/doi/10.4049/jimmunol.0800377

Materials and Methods

Animals and treatment

Twelve-week-old male WT C57BL/6 mice were obtained from Charles River Laboratories. *Mpo*$^{-/-}$ mice were generated by Y. Aratani (Kihara Institute for Biological Research, Kanagawa, Japan) (8) and bred into the C57BL/6 background. Mice were housed individually in standard laboratory cages and allowed food and water ad libitum throughout the experiments. The studies were conducted under a protocol approved by the Institutional Animal Care Committee of Maastricht University.

WT C57BL/6 and *Mpo*$^{-/-}$ mice ($n = 6$ per group) were anesthetized with an i.p. injection of 75 mg/kg ketamine (Nimatek) and 3 mg/kg xylazine (Sedamun). Acute lung inflammation was induced by intratracheal instillation of 20 μg LPS (*Escherichia coli*, serotype O55:B5; Sigma-Aldrich) dissolved in 50 μl of sterile 0.9% NaCl as described previously (9). Sham mice were instilled with 50 μl of LPS-free sterile 0.9% NaCl. After intratracheal instillation, mice were kept in an upright position for 10 min to allow the fluid to spread throughout the lungs. Mice were killed 1, 2, 3, 4, or 5 days after LPS instillation using 115 mg/kg sodium pentobarbital (Ceva Sante Animale) administered i.p. Right lung lobes were removed and snap frozen in liquid nitrogen. Left lung lobes were prepared for immunohistochemistry as described below. Separate animals were used for collection of BALF and neutrophil isolation.

Myeloperoxidase activity assay

MPO activity was determined using a myeloperoxidase assay kit (CytoStore) according to manufacturer's protocol. Briefly, ~50 μg of snap frozen lung from LPS- and sham-treated animals was homogenized in 1 ml of cold sample buffer and centrifuged at 4°C for 5 min at 14,000 rpm. MPO activity was determined in 20 μl of supernatants in duplicate using development reagent. Activity was measured over 25 s at 450 nm. Development reagent without sample was used as a control.

Immunohistochemistry

After thoracotomy, the left lung was inflated with 10% zinc-buffered formalin (pH 5.5) at a pressure of 20 cm H_2O through the trachea and subsequently fixed in 10% zinc-buffered formalin for 24 h. After paraffin embedding, 4-μm sections were cut and mounted on slides. Lung sections from sham and LPS-exposed mice were deparaffinized and endogenous peroxidase activity quenched.

MPO localization

Sections were blocked using 20% (v/v) normal swine serum in TBS for 30 min. MPO was detected using a polyclonal rabbit anti-MPO Ab (0398; DAKO) followed by an anti-rabbit biotin labeled secondary Ab (E0413; DAKO). Labeling was visualized using avidin-biotin peroxidase (K0377; DAKO) and histogreen (Linaris).

CD3 staining for detection of T cells

Ag retrieval was performed by microwave treatment in 10 mM citrate buffer (pH 6.0) followed by 30 min blocking in 10% (v/v) FCS. CD3 was detected with a rat anti-human CD3 Ab (CD3–12; Serotec) followed by a biotin-labeled anti-rat secondary Ab (E0467; DAKO), in turn followed by streptavidin-labeled HRP (P0397; DAKO). Staining was visualized with 3,3′-diaminobenzidine (D4168; Sigma-Aldrich).

B220-staining for detection of B cells

Ag retrieval was performed by means of proteinase K (S3020; DAKO) incubation, followed by blocking for 30 min in 10% (v/v) FCS. B220 was detected with a monoclonal rat anti-B220 Ab (RA3–6B2; BD Pharmingen), followed by a biotin-labeled anti-rat secondary Ab (E0467; DAKO) in turn followed by streptavidin-labeled HRP (P0397; DAKO). Staining was visualized using DAB.

Quantification of cellular influx in lung tissue

H&E-stained sections were used to quantify infiltration of neutrophils and macrophages into the lung. CD3- and B220-stained sections were used to quantify infiltration of lymphocytes and B cells, respectively. At a magnification of 200×, random fields were selected and the number of infiltrated still intact cells was counted. At least five fields per section were analyzed.

Quantitative PCR (Q-PCR) detection of ho-1 *expression*

Total lung RNA was isolated using the RNeasy Mini kit (Qiagen) according to manufacturer's protocol. Total RNA was reverse transcribed, using the Abgene kit with random decamers and oligo(dT) primers and with cDNA amplified by real-time PCR using MyIQ5 (Bio-Rad) with the following primers: *ho-1* (forward) 5′-CCGCCTTCCTGCTCAACAT-3′, (reverse) 5′-CATCTGTGAGGGACTCTGGTCTT-3′; *Calnexin* (forward) 5′-GCAGCGACCTATGATTGACAACC-3,(reverse)5′-GCTCCAAACCAA TAGCACTGAAAGG-3′. Each PCR contained 1× SYBR Green PCR master mix (Applied Biosystems) and 0.3 μM each of forward and reverse primer. Following an initial 10-min incubation at 95°C, thermal cycling was performed using 45 cycles of 94°C for 15 s, 60°C for 30 s and 72°C for 30 s. Gene expression was quantified using standard curves for the respective cDNA products. All changes in *ho-1* cDNA levels were normalized to changes in *calnexin* cDNA as a housekeeping gene.

Table I. *Genes and respective assay IDs for the predesigned TaqMan probe and primer sets*

Genes	Assay IDs
Cytokine receptors	
TNFr1a	Mm00441875_m1
TNFr1b	Mm00441889_m1
Chemokine Receptors	
CCR1	Mm00438260_s1
CXCR1	Mm00731329_s1
CXCR2	Mm00438258_m1
TLRs	
TLR-4	Mm00445274_m1
Cytokines	
IL-6	Mm00446190_m1
TNF-α	Mm00443258_m1
IL-10	Mm00439616_m1
IL-1β	Mm00434228_m1
Chemokines	
MIP-1α	Mm00441258_m1
KC	Mm00433859_m1
RANTES	Mm01302428_m1
MIP-2	Mm00436450_m1
MCP-1	Mm00441242_m1
Housekeeping	
GAPDH	Mm99999915_g1

Taqman gene expression assay

Q-PCR amplifications were performed according to manufacturer's protocol on an ABI Prism 7900HT sequence detection system (Applied Biosystems) using 384-well plates precoated with Taqman primer/probes purchased from Applied Biosystems (low density array format). Table I shows the genes and respective assay IDs for the predesigned TaqMan probe and primer sets (Applied Biosystems) used. The binding probes were 5′-labeled with a 6-carboxyfluorescein dye and a nonfluorescent quencher at the 3′ end. All assays span exon-intron boundaries and cover the major transcript forms. cDNA (10 μl) was mixed with 40 μl nuclease-free water and 50 μl of TaqMan Universal PCR master mix. Sample-specific PCR mixture (100 μl) was loaded into one sample port. The cards were centrifuged twice for 1 min at 1200 rpm and sealed to prevent well-to-well contamination. The cards were placed in the Micro Fluidic card sample block of an ABI Prism 7900 HT sequence detection system (Applied Biosystems). The thermal cycling conditions were 2 min at 50°C and 10 min at 94.5°C, followed by 40 cycles of 30 s at 97°C and 1 min at 59.7°C. Relative quantification of gene expression was calculated on the expression of the house keeping gene *gapdh*, according to the comparative Ct method ($\Delta Ct = Ct_{\text{gene of interest}} - Ct_{gapdh}$). Comparison of gene expression in different samples was performed based on the differences in ΔCt of individual samples ($\Delta\Delta Ct$).

Bio-Plex analysis of cytokines and chemokines

To quantify cytokine and chemokine levels in BALF and in neutrophil supernatants in vitro, a multiplex suspension protein array was performed using the Bio-Plex protein array system and a mouse cytokine 23-plex panel (Bio-Rad) (10). This method of analysis is based on Luminex technology and simultaneously measures IL-1α, IL-1β, IL-2, IL-3, IL-4, IL-5, IL-6, IL-9, IL-10, IL-12(p40), IL-12(p70), IL-13, IL-17, TNF-α, RANTES, MIP-1α, MIP-1β, MCP-1, KC, G-CSF, GM-CSF, IFN-γ, and eotaxin protein. In brief, anti-cytokine/chemokine Ab-conjugated beads were added to individual wells of 96-well filter plate and adhered using vacuum filtration. After washing, 50 μl of prediluted

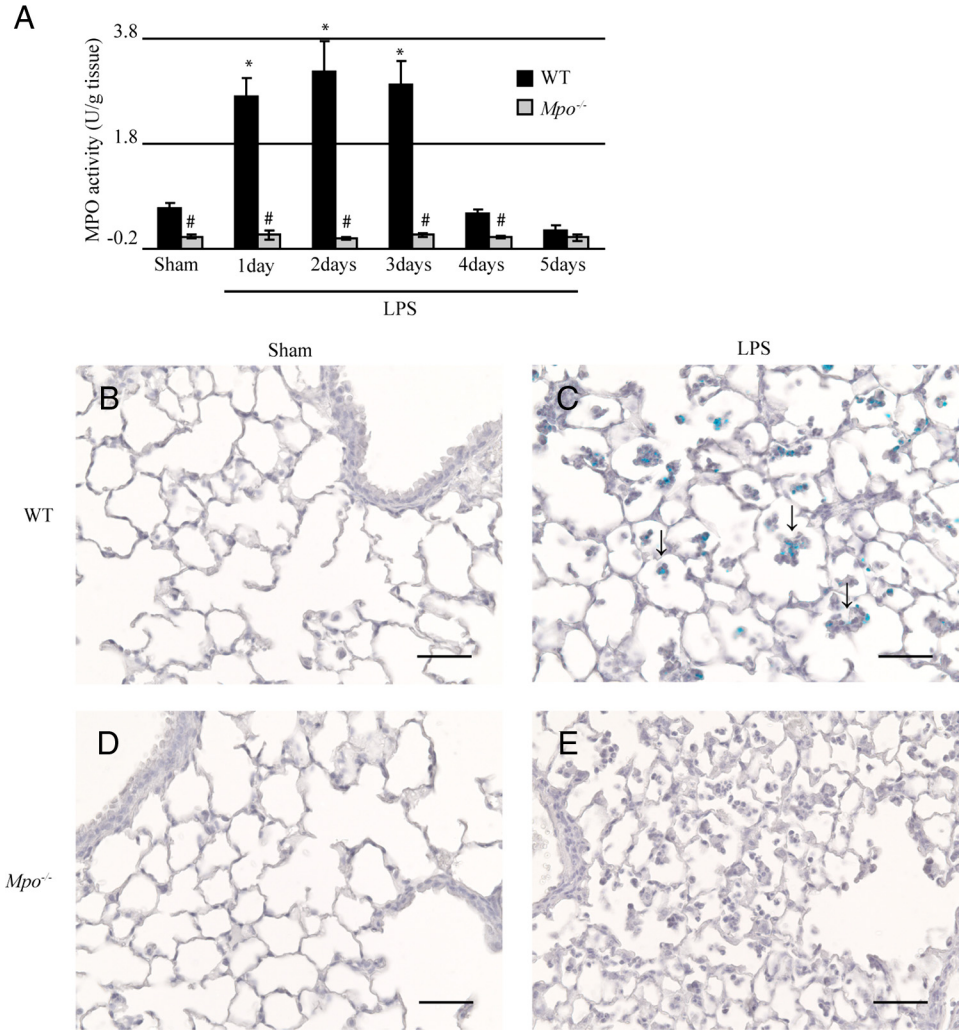

FIGURE 1. *A*, Increases in MPO activity in whole lung homogenates from LPS-exposed WT, but not *Mpo*$^{-/-}$ mice. MPO activity increased rapidly after LPS instillation and returned to baseline levels by day 4. Absence of MPO activity in sham and LPS-exposed *Mpo*$^{-/-}$ mice confirms their knockout status. Values are represented as mean ± SEM. ∗, $p \leq 0.05$ compared with respective sham group; #, $p \leq 0.05$ compared with LPS-exposed WT mice. *B*, LPS exposure increases MPO levels in WT mouse lungs are increased after LPS exposure and MPO is localized in clusters of infiltrating neutrophils (blue stain). Paraffin sections of sham and LPS-exposed WT and *Mpo*$^{-/-}$ mice were stained for MPO. *B*, Sham WT. *C*, LPS WT. *D*, Sham *Mpo*$^{-/-}$. *E*, LPS-exposed *Mpo*$^{-/-}$ mice lack MPO staining. Bars = 50 μm.

standards (range: 1.95–32,000 pg/ml) or plasma samples were added and the filter plate shaken at 300 rpm. Thereafter, the filter plate was washed and 25 μl of prediluted multiplex biotin-conjugated Ab was added. After washing, 50 μl of prediluted streptavidin-conjugated PE was added, followed by an additional wash and the addition of 125 μl of Bio-Plex buffer to each well. The filter plate was analyzed using the Bio-Plex protein array system and concentrations of each cytokine and chemokine were determined using Bio-Plex Manager version 3.0 software.

Neutrophil isolation

Neutrophils were isolated from whole blood of WT and *Mpo*$^{-/-}$ control mice. Mice were euthanized with 115 mg/kg sodium pentobarbital followed by cardiac puncture to collect whole blood with anti-coagulant. Collected blood was diluted in 4 ml of PBS and 5 ml of lysis buffer (155 mM NH_4Cl, 10 mM $NaHCO_3$, pH 7.3) and subsequently incubated on ice for 10 min. White blood cells were spun down by centrifugation for 10 min at 400 × *g* and cells from three mice were pooled in PBS-0.5% BSA. Immunomagnetic isolation of the neutrophils was performed using the anti-Ly-6G microbead kit (Miltenyi Biotec) according to the manufacturer's protocol. Cell viability was confirmed with the trypan blue exclusion assay. Cultures were over 95% pure and viable. Isolated neutrophils were resuspended in RPMI 1640 (Life Technologies) containing 10% FBS for chemotaxis assays or culture.

Neutrophil chemotaxis assay

Neutrophils were resuspended to a final concentration of 3.5×10^5 cells/ml. Cell migration was assayed in a 10-mm Transwell chamber system (Nunc) with 3.0-μm pore polycarbonate filters. Neutrophils were added to the upper compartment and culture medium with or without KC (10 mM; PeproTech) added to the lower compartment. Cell migration was analyzed after 60 min by counting the number of migrated cells in 20 μl with a hemocytometer.

Neutrophil in vitro cytokine and chemokine production

Neutrophils were resuspended to a final concentration of 5×10^5 cells/ml and seeded in a 96-well plate, followed by stimulation with LPS (10 μg/ml) for 24 h. Cell culture supernatants were collected and cytokine and chemokine levels were determined using the Bio-Plex analysis as described above.

Statistical analysis

Data were reported as mean ± SEM. Results from in vivo experiments were analyzed using the Mann-Whitney *U* test, and the results from in vitro experiments were analyzed using ANOVA. Values of $p \leq 0.05$ between groups were considered significant.

Results

Development of acute lung inflammation after intratracheal LPS instillation

To determine MPO activity at each time point during inflammation and to confirm *Mpo*$^{-/-}$ status, total MPO activity was determined in lung tissue of WT and *Mpo*$^{-/-}$ mice after LPS exposure. Fig. 1*A* shows a time-dependent increase in MPO activity after LPS exposure in WT animals. MPO activity peaks 2–3 days after instillation and decreases to control levels after 4 days. *Mpo*$^{-/-}$ mice do not demonstrate MPO activity.

To localize MPO in the lungs of WT animals and to confirm the absence of MPO activity in *Mpo*$^{-/-}$ mice, sections were stained

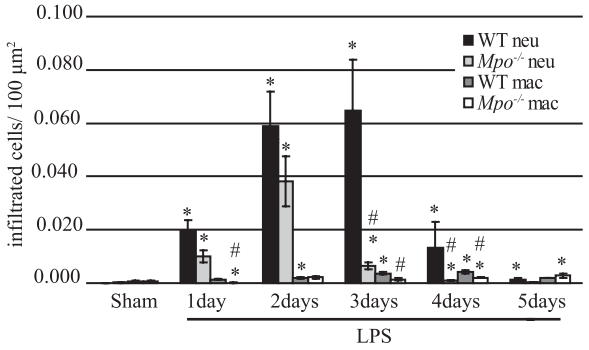

FIGURE 2. Reduced inflammation after LPS exposure in lungs of $Mpo^{-/-}$ mice lungs compared with WT mouse lungs. Quantification of cellular influx on stained paraffin sections demonstrated an inflammatory peak at 2–3 days postexposure. Values are represented as mean ± SEM. ∗, $p \leq 0.05$ compared with respective sham; #, $p \leq 0.05$ compared with LPS-exposed WT mice. Neu, neutrophil; mac, macrophage.

for MPO. WT animals exposed to LPS showed MPO staining in neutrophil clusters through out the lung (Fig. 1*C*). No MPO staining occurred in WT sham (Fig.1*B*) nor in sham or LPS-exposed $Mpo^{-/-}$ mouse lungs (Fig. 1, *D* and *E*).

Consistent with MPO activity data, in Fig. 2 we demonstrate a striking increase in neutrophil influx in WT mice that peaks at 3 days postexposure and returns to control levels at 5 days postexposure. LPS-exposed $Mpo^{-/-}$ mice show a striking decrease in neutrophil influx compared with WT mice. Moreover, compared with WT mice, lung neutrophilia in $Mpo^{-/-}$ mice peaks earlier, namely 2 days postexposure, and returns to control levels by day 5. LPS instillation also resulted in an increase of infiltrating macrophages in WT and $Mpo^{-/-}$ mice that peaked at 4 days postexposure in WT mice. In $Mpo^{-/-}$ mice, the influx was generally lower but persisted over a longer period. The influx of B cells and lymphocytes in response to LPS was negligible (data not shown).

Increased ho-1 *mRNA in LPS-exposed WT and* Mpo$^{-/-}$ *mice*

Ho-1 mRNA expression was examined in whole lung RNA of LPS-exposed WT and $Mpo^{-/-}$ mice as a general marker of oxidative stress. LPS induced an increase in *ho-1* expression in WT and $Mpo^{-/-}$ mouse lungs (Fig. 3*A*) that was significant from sham groups at all times. $Mpo^{-/-}$ mice showed similar *ho-1* expression levels compared with WT mice. However, the expression of *ho-1* relative to the amount of neutrophil infiltration in lung was higher in $Mpo^{-/-}$ than in WT mice (Fig. 3*B*).

Mpo$^{-/-}$ *mice show normal expression of inflammatory receptor genes*

Possible knockout effects on expression patterns of several receptors known to be important in the development of lung inflammation were investigated by Q-PCR. TLR-4, TNF receptor-1α and -1β, *ccr-1*, and *cxcr-2* mRNA levels were not different in sham-treated WT and $Mpo^{-/-}$ mice (data not shown). In contrast to what would be expected, *cxcr-1* expression was significantly increased in sham-treated $Mpo^{-/-}$ mice compared with WT mice.

Mpo$^{-/-}$ *mice show altered patterns of inflammation-associated cytokines and chemokines*

The induction of cytokines and chemokines was determined on mRNA levels 2 days postexposure and protein levels were determined 3 days postexposure in BALF. Fig. 4 demonstrates a significant increase in mRNA expression of neutrophil and macrophage chemotactic proteins IL-6, KC, MIP-1α, and RANTES after LPS in WT mice. mRNA expression levels of KC and RANTES were significantly reduced in $Mpo^{-/-}$ after LPS compared with WT mice. Of the investigated cytokines and chemokines, TNF-α,

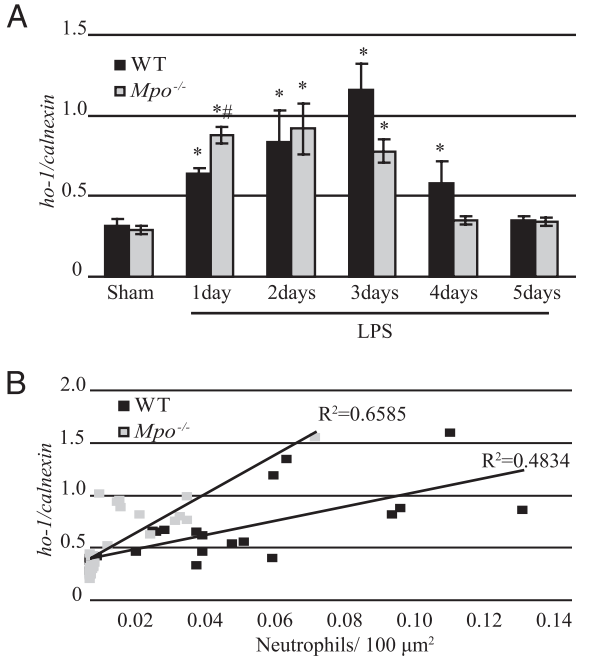

FIGURE 3. LPS instillation results in increased mRNA expression of *ho-1* in WT and $Mpo^{-/-}$ mice. *A*, Whole lung mRNA was isolated and *ho-1* expression was analyzed by Q-PCR and normalized against *calnexin* expression. *Ho-1* expression increased after LPS instillation but similar levels were found in WT and $Mpo^{-/-}$ mice. Values are represented as mean ± SEM. *B*, *Ho-1* expression correlated with number of infiltrating neutrophils but the expression of *ho-1* relative to neutrophil infiltration was higher in $Mpo^{-/-}$ mice than in WT. ∗, $p \leq 0.05$ compared with respective sham; #, $p \leq 0.05$ compared with LPS-exposed WT mice.

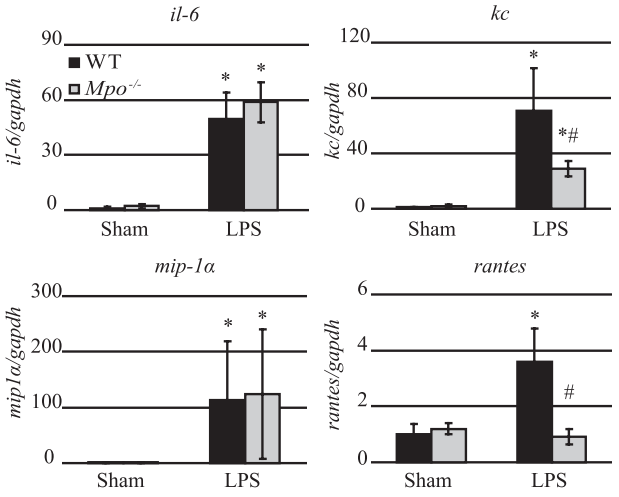

FIGURE 4. $Mpo^{-/-}$ mice show altered mRNA expression levels of various cytokines/chemokines compared with WT mice after LPS instillation. Cytokine and chemokine expression levels were measured in whole lung mRNA 2 days after LPS exposure, as described in *Materials and Methods*. Values are represented as mean ± SEM. ∗, $p \leq 0.05$ compared with respective sham; #, $p \leq 0.05$ compared with LPS-exposed WT mice.

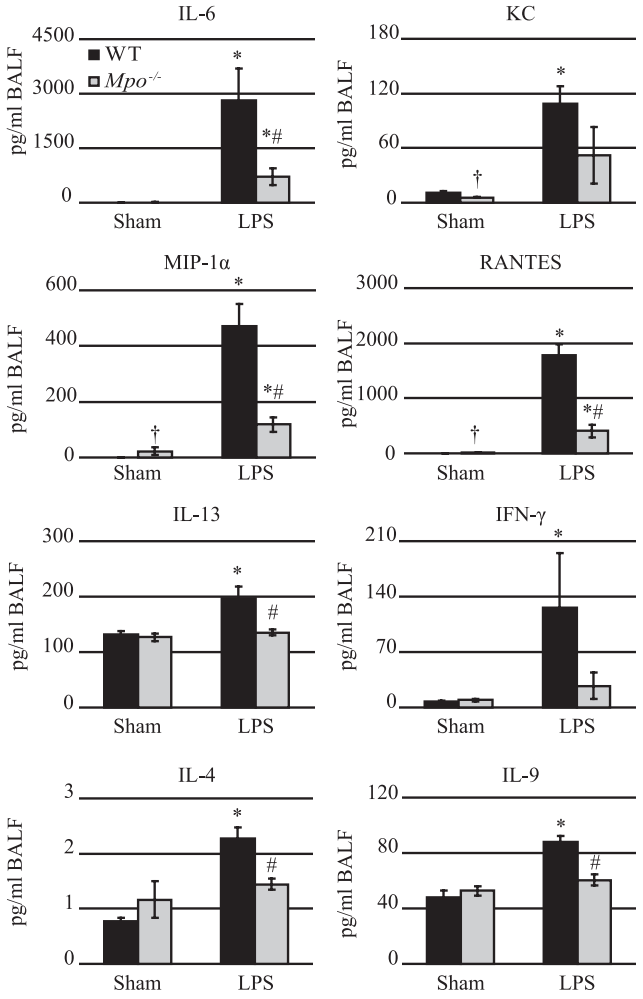

FIGURE 5. $Mpo^{-/-}$ mice demonstrate altered cytokine/chemokines protein levels compared with WT mice after LPS instillation. Cytokine and chemokine protein levels were measured in BALF 3 days after LPS exposure, as described in *Materials and Methods*. Values are represented as mean ± SEM. *, $p \leq 0.05$ compared with respective sham; #, $p \leq 0.05$ compared with LPS-exposed WT mice; †, $p \leq 0.05$ compared with WT sham.

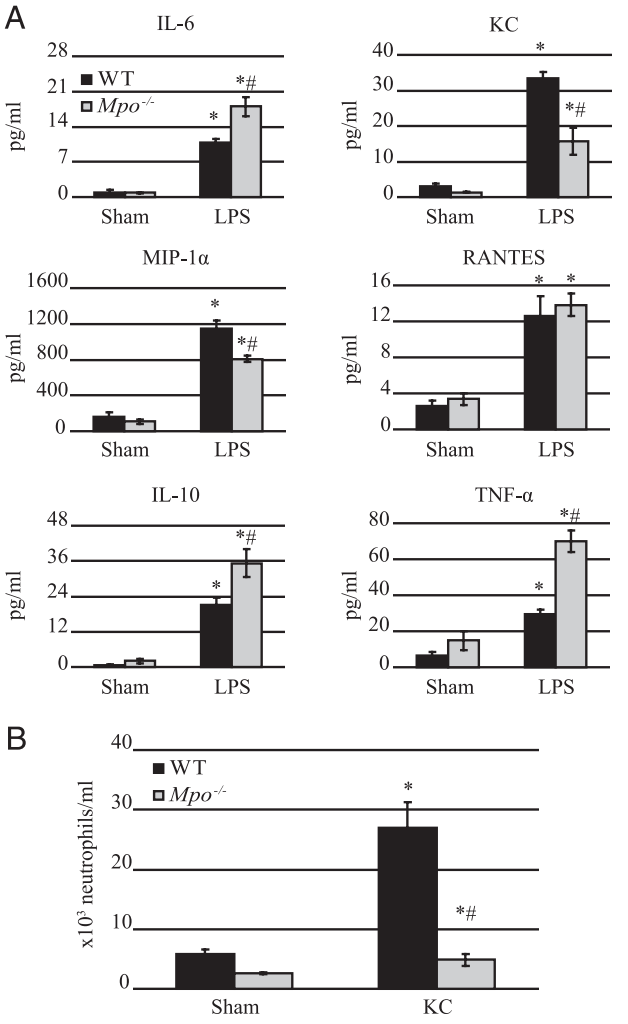

FIGURE 6. $Mpo^{-/-}$ neutrophils in vitro show altered production of cytokines and chemokines compared with WT neutrophils and decreased migration. *A*, Cytokine and chemokine protein levels were measured in cell culture supernatant of isolated WT and $Mpo^{-/-}$ neutrophils 24 h after LPS stimulation, as described in *Materials and Methods*. *B*, $Mpo^{-/-}$ neutrophils demonstrate decreased migration toward a KC gradient compared with WT neutrophils. Values are represented as mean ± SEM. *, $p \leq 0.05$ compared with respective sham; #, $p \leq 0.05$ compared with LPS-exposed WT neutrophils.

IL-1β, IL-10, MCP-1 and MIP-2 showed a significant increase in mRNA expression after LPS exposure, but knockout effects were not observed (data not shown). Although mRNA expression levels of IL-6 and MIP-1α were not reduced in $Mpo^{-/-}$ mice, Fig. 5 shows that protein levels of IL-6 and MIP-1α were significantly reduced in $Mpo^{-/-}$ mice compared with WT mice. IL-13, capable of inhibiting IL-6 and KC, was decreased in $Mpo^{-/-}$ mice compared with WT mice, as was the neutrophil and macrophage activity promoting cytokine IFN-γ. In line with these results, a significant decrease of the blood monocyte chemoattractant RANTES was observed in $Mpo^{-/-}$ mice after LPS exposure. IL-4 and IL-9 were also significantly decreased in $Mpo^{-/-}$ mice after LPS exposure compared with WT mice. Of the panel of 23 cytokines and chemokines measured in BALF, IL-1α, IL-1β, IL-3, IL-10, IL-12(p40), IL-12(p70), IL-17, MIP-1β, MCP-1, G-CSF, GM-CSF, and eotaxin were all elevated in BALF after LPS exposure in WT and $Mpo^{-/-}$ mice (data not shown). IL-2 protein levels showed a slight decrease after LPS exposure (data not shown). Protein concentrations of IL-5 and TNF-α in BALF in response to LPS were not different from control levels at day 3 in WT and $Mpo^{-/-}$ mice (data not shown).

Mpo$^{-/-}$ *neutrophils show altered cytokine and chemokine production and decreased migration in vitro*

Analysis of supernatants of LPS-exposed WT and $Mpo^{-/-}$ neutrophils demonstrated very low amounts of IL-6, KC, and RANTES protein (Fig. 6*A*). These levels were increased after LPS exposure in WT and $Mpo^{-/-}$ neutrophil supernatants. KC and MIP-1α showed similar patterns in vitro and in vivo. IL-6 levels were opposite to those in BALF, with increased levels in $Mpo^{-/-}$ neutrophil supernatant. Of the panel of 23 cytokines and chemokines measured, IL-2, IL-3, IL-4, IL-5, IL-9, IL-12(p40), IL-13, IL-17, MCP-1, and IFN-γ were not detectable and GM-CSF and eotaxin levels were not altered by LPS exposure (data not shown). IL-1α, IL-1β, MIP-1β, IL-12(p70), and G-CSF were elevated after LPS exposure in WT and $Mpo^{-/-}$ mice (data not shown). IL-10 and TNF-α levels increased significantly after LPS exposure and were even further elevated in the supernatants of $Mpo^{-/-}$ compared with WT neutrophils.

To determine whether decreased neutrophilic inflammation could be due to decreased migration of $Mpo^{-/-}$ neutrophils, a

chemotaxis assay was performed with isolated WT and *Mpo*$^{-/-}$ neutrophils. Migration toward a KC gradient decreased in *Mpo*$^{-/-}$ neutrophils compared with WT neutrophils (Fig. 6*B*).

Discussion

MPO is an important enzyme in innate defense, because it produces hypochlorous acid (HOCl) and other reactive oxidants (11). This study aimed to investigate the contribution of MPO to LPS-induced lung inflammation and subsequent effects on cytokine and chemokine production. We report a significantly decreased neutrophilia in *Mpo*$^{-/-}$ mice, compared with WT animals, that peaks 2 days after LPS exposure. WT mice revealed an inflammatory peak 2–3 days postexposure that returned to control levels 5 days postexposure. This decrease in neutrophil influx in *Mpo*$^{-/-}$ mice confirms our previous work demonstrating decreased neutrophil levels in BALF of *Mpo*$^{-/-}$ compared with WT mice after chrysotile asbestos exposure (7). A similar early peak in neutrophilia, as we report in this paper, has been shown before in *Mpo*$^{-/-}$ mice in a study on UV-induced skin inflammation (12). In earlier studies by our group, we reported peak neutrophil influx in Swiss mice 1 day after LPS exposure (13). This suggests a strain-dependent time response to intratracheal LPS instillation.

Furthermore, we showed that LPS instillation results in a dramatic increase in MPO activity in WT mice. Moreover, we demonstrate that MPO is predominantly localized in clusters of infiltrated and activated neutrophils. We demonstrated previously in a mouse model of asbestosis that MPO occurred in distal bronchiolar epithelium at alveolar duct bifurcations, site of asbestos fiber deposition (7). This suggests that distribution of MPO within the lung may be disease model dependent.

A significant increase in *ho-1* expression in WT and *Mpo*$^{-/-}$ mice after LPS exposure was observed. The dose of LPS used here resulted in a dramatic lung neutrophilia in WT mice with subsequent oxidative stress. This suggests that compensatory feedback mechanisms like the anti-oxidant marker *ho-1* are upregulated. This dramatic neutrophilia however does not explain why *Mpo*$^{-/-}$ mice show similar patterns of *ho-1* expression as WT mice. Aratani et al. reported on a study comparing *Mpo*$^{-/-}$, NADPH-oxidase$^{-/-}$, and double knockout mice in a model of pulmonary infection that could explain these findings (14). They showed that H_2O_2 used by MPO is solely produced by NADPH-oxidase. Therefore, it is tempting to speculate that *Mpo*$^{-/-}$ mice that are incapable of converting H_2O_2 to HOCl, build up H_2O_2. Increased H_2O_2 levels could explain *ho-1* mRNA expression, because H_2O_2 is a very potent oxidant like HOCl.

Cytokines and chemokines are key players in the recruitment of neutrophils and macrophages to inflammatory sites. We demonstrate that the decreased neutrophilia found in *Mpo*$^{-/-}$ mice exposed to intratracheal LPS is not due to differences in inflammatory receptor expression patterns but due to significantly lower protein levels of the neutrophil attractants KC, IL-6, and MIP-1α in BALF compared with WT mice. The positive contribution of these inflammatory signaling molecules to the development of lung neutrophilia is in line with the literature. The lower levels of neutrophil attractants in the lungs of *Mpo*$^{-/-}$ mice are in contrast to recent work in a model of fungal-induced lung infection where *Mpo*$^{-/-}$ mice demonstrated KC levels comparable to those of WT mice (15). IL-13 has been described to inhibit IL-6 and IL-8 production by human monocytes (16). It is therefore tempting to speculate that decreased protein levels of IL-13 in BALF of *Mpo*$^{-/-}$ are due to decreased IL-6 and KC, the mouse equivalent of IL-8. After neutrophils become apoptotic, macrophages are attracted to phagocytose apoptotic cells and cell debris. RANTES is a chemoattractant for peripheral blood monocytes. Because macrophage numbers were generally lower in *Mpo*$^{-/-}$ mice compared with WT, it is tempting to speculate that this was due to decreased RANTES levels.

In addition to being a neutrophil chemoattractant, MPO itself has been described to play a role in the activation of neutrophils. Lau et al. (6) demonstrated that MPO binds to CD11b/CD18 integrins on neutrophils, leading to induction of intracellular signaling cascades and translating into increased neutrophil degranulation and CD11b surface expression. CD11b/CD18 is a critical mediator for neutrophil adherence before extravasation. We show that decreased early neutrophilia is mainly a result of decreased extravasation and decreased chemoattractant production is a result of this, although a small fraction of the decreased KC and MIP-1α levels could be due to a decreased production by *Mpo*$^{-/-}$ neutrophils.

In summary, our results show that MPO activity is increased after LPS-exposure. MPO localizes in clusters of infiltrated and activated neutrophils of LPS-exposed WT mice. Neutrophil influx in LPS-exposed *Mpo*$^{-/-}$ mice is significantly decreased compared with WT mice, predominantly as a result of decreased migration of *Mpo*$^{-/-}$ neutrophils. *Ho-1*-expression levels increased after LPS exposure but were similar in WT and *Mpo*$^{-/-}$ mice. LPS-exposed *Mpo*$^{-/-}$ mice demonstrated an altered pattern of inflammatory cytokine and chemokine expression that is not due to their altered production by *Mpo*$^{-/-}$ neutrophils per se. These data suggest that MPO not only plays an important role in the development of lung neutrophilia but also indirectly contributes to chemokine and cytokine production that may govern inflammatory processes.

Acknowledgments

We thank Betty van der Veen (Department of Pathology and Laboratory Medicine, University Medical Center Groningen, Groningen, The Netherlands), Nadja Drummen, Claudia Geijselaers (Department of Respiratory Medicine, Maastricht uMC+, Maastricht, The Netherlands) and Peter Frings (Department of Internal Medicine, Division of Hematology, Lab for Tumor Immunology, Maastricht uMC+, The Netherlands) for their excellent assistance.

Disclosures

The authors have no financial conflict of interest.

References

1. Weiland, J. E., W. B. Davis, J. F. Holter, J. R. Mohammed, P. M. Dorinsky, and J. E. Gadek. 1986. Lung neutrophils in the adult respiratory distress syndrome: clinical and pathophysiologic significance. *Am. Rev. Respir. Dis.* 133: 218–225.
2. Saleh, D., P. J. Barnes, and A. Giaid. 1997. Increased production of the potent oxidant peroxynitrite in the lungs of patients with idiopathic pulmonary fibrosis. *Am. J. Respir. Crit. Care Med.* 155: 1763–1769.
3. Cullen, M. R., and W. W. Merrill. 1992. Association between neutrophil concentration in bronchoalveolar lavage fluid and recent losses in diffusing capacity in men formerly exposed to asbestos. *Chest* 102: 682–687.
4. Hogg, J. C., F. Chu, S. Utokaparch, R. Woods, W. M. Elliott, L. Buzatu, R. M. Cherniack, R. M. Rogers, F. C. Sciurba, H. O. Coxson, and P. D. Pare. 2004. The nature of small-airway obstruction in chronic obstructive pulmonary disease. *N. Engl. J. Med.* 350: 2645–2653.
5. Papi, A., C. M. Bellettato, F. Braccioni, M. Romagnoli, P. Casolari, G. Caramori, L. M. Fabbri, and S. L. Johnston. 2006. Infections and airway inflammation in chronic obstructive pulmonary disease severe exacerbations. *Am. J. Respir. Crit. Care Med.* 173: 1114–1121.
6. Lau, D., H. Mollnau, J. P. Eiserich, B. A. Freeman, A. Daiber, U. M. Gehling, J. Brummer, V. Rudolph, T. Munzel, T. Heitzer, T. Meinertz, and S. Baldus. 2005. Myeloperoxidase mediates neutrophil activation by association with CD11b/CD18 integrins. *Proc. Natl. Acad. Sci. USA* 102: 431–436.
7. Haegens, A., A. van der Vliet, K. J. Butnor, N. Heintz, D. Taatjes, D. Hemenway, P. Vacek, B. A. Freeman, S. L. Hazen, M. L. Brennan, and B. T. Mossman. 2005.

Asbestos-induced lung inflammation and epithelial cell proliferation are altered in myeloperoxidase-null mice. *Cancer Res.* 65: 9670–9677.
8. Aratani, Y., H. Koyama, S. Nyui, K. Suzuki, F. Kura, and N. Maeda. 1999. Severe impairment in early host defense against *Candida albicans* in mice deficient in myeloperoxidase. *Infect. Immun.* 67: 1828–1836.
9. Starcher, B., and I. Williams. 1989. A method for intratracheal instillation of endotoxin into the lungs of mice. *Lab. Anim.* 23: 234–240.
10. Sabo-Attwood, T., M. Ramos-Nino, J. Bond, K. J. Butnor, N. Heintz, A. D. Gruber, C. Steele, D. J. Taatjes, P. Vacek, and B. T. Mossman. 2005. Gene expression profiles reveal increased mClca3 (Gob5) expression and mucin production in a murine model of asbestos-induced fibrogenesis. *Am. J. Pathol.* 167: 1243–1256.
11. Klebanoff, S. J. 1999. Myeloperoxidase. *Proc. Assoc. Am. Physicians* 111: 383–389.
12. Komatsu, J., H. Koyama, N. Maeda, and Y. Aratani. 2006. Earlier onset of neutrophil-mediated inflammation in the ultraviolet-exposed skin of mice deficient in myeloperoxidase and NADPH oxidase. *Inflamm. Res.* 55: 200–206.
13. Vernooy, J. H., M. A. Dentener, R. J. van Suylen, W. A. Buurman, and E. F. Wouters. 2001. Intratracheal instillation of lipopolysaccharide in mice induces apoptosis in bronchial epithelial cells: no role for tumor necrosis factor-αand infiltrating neutrophils. *Am. J. Respir. Cell Mol. Biol.* 24: 569–576.
14. Aratani, Y., F. Kura, H. Watanabe, H. Akagawa, Y. Takano, K. Suzuki, M. C. Dinauer, N. Maeda, and H. Koyama. 2002. Relative contributions of myeloperoxidase and NADPH-oxidase to the early host defense against pulmonary infections with *Candida albicans* and *Aspergillus fumigatus*. *Med. Mycol.* 40: 557–563.
15. Aratani, Y., F. Kura, H. Watanabe, H. Akagawa, Y. Takano, A. Ishida-Okawara, K. Suzuki, N. Maeda, and H. Koyama. 2006. Contribution of the myeloperoxidase-dependent oxidative system to host defence against *Cryptococcus neoformans*. *J. Med. Microbiol.* 55: 1291–1299.
16. Zurawski, G., and J. E. de Vries. 1994. Interleukin 13, an interleukin 4-like cytokine that acts on monocytes and B cells, but not on T cells. *Immunol. Today* 15: 19–26.